Supplementary Information

A Bis-quinoline Ruthenium(II) arene complex with submicromolar cytotoxicity in castration-resistant prostate cancer cells

Author Full Name,[a] Author Full Name,[b] Author Full Name,[C]*

ELECTRONIC SUPPORTING INFORMATION

Contents	
Page S1-S5	Experimental Details
Fig. S1	IR spectrum of **pCYRuL** recorded using KBr disc technique.
Fig. S2	^{1}H-NMR spectrum of **pCYRuL** recorded in DMSO-d_6.
Fig. S3	Aliphatic region of ^{1}H-^{1}H-COSY NMR spectrum of **pCYRuL** recorded in DMSO-d_6.
Fig. S4	Aromatic region of the ^{1}H-^{1}H-COSY NMR spectrum of **pCYRuL** recorded in DMSO-d_6.
Fig. S5	^{13}C-NMR spectrum of **pCYRuL** recorded in DMSO-d_6.
Fig. S6	ESI-Mass spectrum of **pCYRuL** recorded in methanol.
Fig. S7.	UV-Vis absorption spectra of **pCYRuL** [30 μM] recorded in DMSO at 298 K.
Fig. S8	UV-Visible absorption spectra of **pCYRuL** (30 μM) recorded in 4% DMSO-PBS (pH ~ 7.4) after 0, 12, 24 and 48 h at 298 K.
Fig. S9	UV-Visible absorption spectra of **pCYRuL** (30 μM) recorded in DMSO after 0, 12, 24 and 48 h at 298 K.
Fig. S10	^{1}H-NMR spectrum of **pCYRuL** recorded in DMSO-d_6 after 0, 0.5, 2, 6, 12, 24 and 48 h at 298 K.
Fig. S11	Cyclic voltammograms of **pCYRuL** (1 mM) solution in CH_3CN with 0.1 M $[nBu_4N][ClO_4]$ at scan rates: 100 mV s^{-1} at room temperature.
Table S1	Data obtained from the cyclic voltammetry analyses of **pCYRuL** at the scan rate of 100 mV s^{-1}.
Table S2	Cytotoxicity of pCYRuL in different cancer cell lines.
Fig. S12.	Toxicity analysis of pCYRuL in HK2 cells. The tests were conducted in triplicate.
Fig. S13.	Toxicity analysis of pCYRuL in MCF10A cells. The tests were conducted in triplicate.
Fig. S14	Stern-Volmer plot for the calculation of quenching constant (K_{SV}) associated with the titration of EthBr-DNA and **pCYRuL** at 298 K.
Fig. S15	Scatchard plot for the calculation of association constant (K_a) related with the interaction of EthBr-DNA and **pCYRuL** at 298 K.
Table S3.	Data from the emission spectroscopic studies on the DNA binding ability of complexes **1-3**.

Experimental Details:

Materials used

All common chemicals and solvents were purchased from Sigma Aldrich, Thermo-Fisher Scientific, Molychem and CDH, India and used without further purification. Solvents used for spectroscopic and electrochemical analyses were purified and dried by standard methods. Metal chloride ($RuCl_3 \cdot 3H_2O$), α-terpinene, quinaldine, hydrazine, potassium hexafluorophosphate, ethidium bromide (EthBr), phosphate buffer saline (PBS), calf thymus-deoxyribonucleic acid (CT-DNA) and bovine serum albumin (BSA) were procured by Sigma Aldrich and TCI, India. 3-(4,5-dimethylthiazol-2-yl)-2,5-diphenyltetrazolium bromide (MTT) was obtained from Sigma-Aldrich, MO, USA.

Syntheses and characterization

The ligand 1,2-bis(quinolin-2-ylmethylene)hydrazine (**L**) was synthesized using method described in the literature.[1] The Ru(p-cymene) dimer (**P**) were synthesized and purified using methods described in the literature.[2, 3] The complex **(**pCYRuL) was synthesized and purified by the synthetic procedure shown in the Chart 1 of main text.

General procedure for preparation of complex (pCYRuL)

The mixture of Ru(p-cymene)dimer $[((\eta^6\text{-p-cymene})Ru(\mu\text{-}Cl)Cl)_2]$ (**P**) (0.5 mmol) and 1,2-bis(quinolin-2-ylmethylene)hydrazine (**L**) (1.0 mmol) dissolved in dry dichloromethane and dry methanol (1:1 (v/v); 25 mL) was refluxed under nitrogen for 12 h. After completion of the reaction, the solution was cool down to room temperature. A solution of potassium hexafluorophosphate (KPF_6) (1.5 mmol) in dry methanol was added and allowed it to stir at room temperature for 4-5 hours. Solvent was removed under vacuum after completion of reaction.

Characterization of $[(\eta^6$-p-cymene)(L)RuCl]PF_6 (pCYRuL)

The complex pCYRuL was isolated as pure yellowish brown solid by column chromatography using methanol dichloromethane mixture. Yield = 71%. m.p. = 211-213 °C decomp. ^{1}H NMR (500 MHz, DMSO-d_6, δ ppm): 0.87 (3H, d, J = 6.5 Hz, -H_{o1}); 0.99 (3H, d, J = 7 Hz, -H_{o2}); 2.21 (3H, s, -H_k); 3.16-3.17 (1H, m, -H_n); 5.91 (1H, d, J = 5.5 Hz, -H_{m1}); 6.13 (1H, d, J = 5.5 Hz, -H_{m2}); 6.35 (1H, d, J = 5.5 Hz, -H_{l2}); 6.42 (1H, d, J = 6 Hz, -H_{l1}); 7.81 (1H, t, J = 7 Hz, -H_{16}); 7.93 (1H, t, J = 7 Hz, -H_{15}); 8.03 (1H, t, J = 7.5 Hz, -H_7); 8.16-8.23 (3H, m, -$H_{17,8,14}$); 8.32-8.34 (2H, m, -$H_{6,4}$); 8.42 (1H, d, J = 8.5 Hz, -H_{19}); 8.68 (1H, d, J = 8.5 Hz, -H_{20}); 8.74 (1H, d, J = 9 Hz, -H_9); 8.93 (1H, d, J = 8 Hz, -H_3); 9.23 (1H, s, -H_{11}); 9.31 (1H, s, -H_1). ^{13}C NMR (125 MHz, DMSO-d_6, δ ppm): 164.1, 163.0, 154.7, 151.2, 149.0, 148.1, 141.3, 138.1, 133.9, 131.3, 130.8, 130.1, 129.8, 129.6, 129.5, 129.4, 128.7, 124.8, 119.7, 106.5, 105.0, 87.1, 86.7, 85.9, 31.1, 22.5, 21.6, 18.7. Anal. Calcd. (%) for $C_{30}H_{28}ClF_6N_4PRu$: C, 49.63; H, 3.89; N, 7.72. Found (%): C, 49.52; H, 3.86; N, 8.01. ESI-MS(+) in CH_3OH (Calcd, found, *m/z*) 581.1046, 581.1045, $[M]^+$ = [**pCYRuL**-PF_6]$^+$. FTIR (KBr,

cm^{-1}) $\tilde{\nu}$(C-H aromatic+aliphatic) 3440.93, 3073.31, 2924.43, 2862.14, $\tilde{\nu}$(C=N) 1591.85, 1510.78, $\tilde{\nu}$(C=C) 1467.46, 1377.59, $\tilde{\nu}$(PF6) 839.38, $\tilde{\nu}$(Ru-N) 557.08, 509.06, $\tilde{\nu}$(Ru-Cl) 478.89. UV-Vis: (in DMSO), λ_{max} (nm) (ϵ, $dm^3mol^{-1}cm^{-1}$): 349 (2.21×10^4), 445 (5.21×10^3); (in 4 % DMSO:PBS (pH = 7.4)) λ_{max} (nm): 252, 346, 432.

Physical measurements

The melting point was measured using the Büchi Melting Point B-540 apparatus. Infrared spectra were recorded at room temperature using a Perkin Elmer FTIR spectrometer in 4000-400 cm^{-1} range. Conductivity measurements were carried out using the Systronics Conductivity Meter 304. Elemental analysis was performed on a Thermo Scientific Flash 2000 elemental analyzer. The ^1H, ^{13}C and COSY NMR spectra were recorded in DMSO-d_6 and $CDCl_3$ solvents on a Bruker Avance III-500 MHz spectrometer at 298 K. One ^{13}C NMR spectrum was recorded on a Jeol 400 MHz spectrometer at 298 K. UV-Vis spectrophotometric studies were performed at room temperature on an Agilent Technologies Cary 60 UV-Vis spectrophotometer. ESI-mass spectra were recorded on Thermo exactive plus mass spectrometer. Fluorescence studies were conducted using an Agilent Cary Eclipse fluorescence spectrophotometer at 298 K. Cyclic voltammetry experiments were carried out on an AUTOLAB PGSTAT 302N (Metrohm Autolab B.V., Netherlands) electrochemical analyzer.

UV-Visible spectroscopy

UV-Visible data were recorded after 0, 12, 24, and 48 hours using an Agilent Technologies Cary 60 UV-Vis spectrophotometer at 298 K. The stock solutions (30 μM) of complex **pCYRuL** and Ru(arene) precursor **P** was prepared both in 4% DMSO-PBS (pH ~ 7.4) mixture and DMSO for the stability studies.

Cyclic voltammetry

Cyclic voltammetry experiments were carried out on an AUTOLAB PGSTAT 302N (Metrohm Autolab B.V., Netherlands) electrochemical analyzer. A three-electrode system, consisting of glassy carbon as the working electrode (GCE), a platinum-wire as the auxiliary electrode and a silver wire as the pseudo-reference electrode was used for cyclic voltammetric measurements. The electrochemical properties of complex **pCYRuL** was studied in CH_3CN with 0.1 M tetrabutylammoniumperchlorate (TBAP), as the supporting electrolyte.[4] The GCE, 3 mm diameter, was manually polished with a 0.3 μm Al_2O_3 slurry on a polishing cloth, rinsed with double distilled water followed by CH_3CN and dried with argon. All solutions were purged with pure argon prior to measurement to remove oxygen. All electrochemical measurements were carried out by maintaining a blanket of argon over the solutions at room temperature.

Anticancer activity

Human prostatic adenocarcinoma cell line PC-3, hepatocellular carcinoma cell line HepG2 and cells were procured from National Centre for Cell Sciences (NCCS), Pune, India. Human Kidney 2(HK2) cells were obtained from ATCC. The PC3 and HepG2 cells were grown in Roswell Park Memorial Institute Medium, RPMI (Sigma Aldrich, USA) and Dulbecco's Modified Eagle Medium, (Gibco) respectively supplemented with 10% Fetal Bovine Serum (Gibco) and 1% penicillin/streptomycin (Gibco) in 5% CO_2, humidified incubator at 37°C and were maintained using standard cell culture protocols. HK2 cell and Dulbecco's Modified Eagle Medium, (Gibco) respectively supplemented with 20% Fetal Bovine Serum (Gibco) and 1% penicillin/streptomycin (Gibco) in 5% CO_2, humidified incubator at 37°C were maintained using standard cell culture protocols. The stock concentration of **pCYRuL** was prepared in DMSO (Sigma Aldrich) and working dilutions were dissolved in the respective cell culture medium with less than 0.5% DMSO concentration. The cells were seeded (10000 cells/ well) in a 96-well plate followed by a two-fold serial dilution treatment of compounds after 24 hours of incubation. Non-treated control cells were also maintained in the same conditions to compare the growth inhibition. The content in all respective wells including tests and control were decanted after 72 hours of treatment and reconstituted in 10µl of MTT reagent (0.5mg/ml concentration) (Sigma). After 2 hours of dark incubation in a 5% CO_2 humidified incubator, the supernatant was removed and 100 mL of MTT solubilisation solution (DMSO) was added and kept in a shaking incubator at 37ºC to solubilize formazan crystals. The absorbance was recorded at 570nm using a microplate reader. The IC_{50} value was analysed using GraphPad prism 8. All the experiments were performed in biological triplicates.

Cell cycle arrest studies

Human prostatic adenocarcinoma cell line PC-3 cells (1 x 10^6 cells/well) were seeded on 6-well plate for 24 hours incubation followed by treatment with **pCYRuL** at the specified concentrations. After 24 hours treatment, cells were harvested and washed with PBS (1X) (Gibco) followed by fixing cells with drop-by-drop addition of ethanol to a final concentration of 70% and incubated for at two hours. After fixation, cells were centrifuged for 5 mins at 600g; washed with PBS (1X), and subsequently subjected to RNase (100µg/mL) and Propidium Iodide (50µg/mL) labelling solution. Cells were incubated for 15 mins in dark and analysed by Flow Cytometry. All experiments were performed in biological triplicates.

Apoptosis

The apoptosis assay was performed using eBioscience™ Annexin V-FITC Apoptosis Detection Kit (Invitrogen) and analysed by FACS BD-Accuri™. Human prostatic adenocarcinoma cell line PC-3 cells (1 x 10^6 cells/well) were seeded on 6-well plate for 24 hours incubation followed by treatment

with the **pCYRuL**. After 24 hours treatment, cells were harvested, washed with PBS (1X) followed by second washing with binding buffer (1X). The cell pellet was resuspended in 200µL binding buffer (1X) and add 5µl of annexin V-FITC to the cell suspension. The suspension was incubated for 15 minutes at room temperature. The cells were washed and the pellet was resuspended in 200µL binding buffer (1X) and followed by addition of 5ul of Propidium Iodide (20µg/ml). All experiments were performed in biological triplicates.

Emission spectral studies for DNA interaction

In order to examine the interaction of **pCYRuL** with CT-DNA, well known ethidium bromide (EthBr) competition assays were performed. EthBr is a well-known DNA intercalator, which shows weak fluorescence in its free-state. The ability of EthBr to intercalate into the DNA helix allows it to show strong fluorescence in the bound state with CT-DNA.[5, 6] Our experiment showed significant quenching in the fluorescence intensity of the DNA-EthBr complex with increasing concentrations of **pCYRuL** in 4% DMSO-PBS (pH ~ 7.4). This was likely due to the displacement of EthBr from the EthBr-DNA complex. The EthBr-DNA complex was excited at 480 nm, and the emission intensity was monitored at 607 nm. The DNA-EthBr quenching studies for **pCYRuL** were performed following the Stern-Volmer equation:[7-11]

$$F_o / F = K_{sv} [Q] + 1$$

Where F_o and F are the emission intensities of EthBr-DNA in the absence and presence of **pCYRuL**, respectively, K_{sv} is the quenching constant and [Q] is the concentration of **pCYRuL**. In order to verify results obtained from Stern-Volmer equation, data was also plotted using the modified Stern-Volmer or Scatchard equation:

$$\log ((F_o – F) / F) = \log K_a + n \log[Q]$$

Where, K_a is the association constant. The values of K_{sv}, K_a and n for **pCYRuL** were calculated using the above equations. EthBr displacement fluorescence experiments were carried out on an Agilent Cary Eclipse fluorescence spectrophotometer. Fixed concentration solutions of CT-DNA (35 µM) and EthBr (35 µM) were prepared in PBS buffer (pH ~ 7.4). After intercalation of EthBr with DNA, the EthBr-DNA complex showed good fluorescence intensity. The addition of increasing concentrations of complex 0-139 µM (for **pCYRuL**; 4% DSMO-PBS buffer, pH ~ 7.4) showed significant quenching in fluorescence intensity at 298 K. The fluorescence spectral changes were observed at the excitation wavelength ($\lambda_{ex.}$) and the emission wavelength (λ_{em}), 480 nm and 607 nm, respectively.

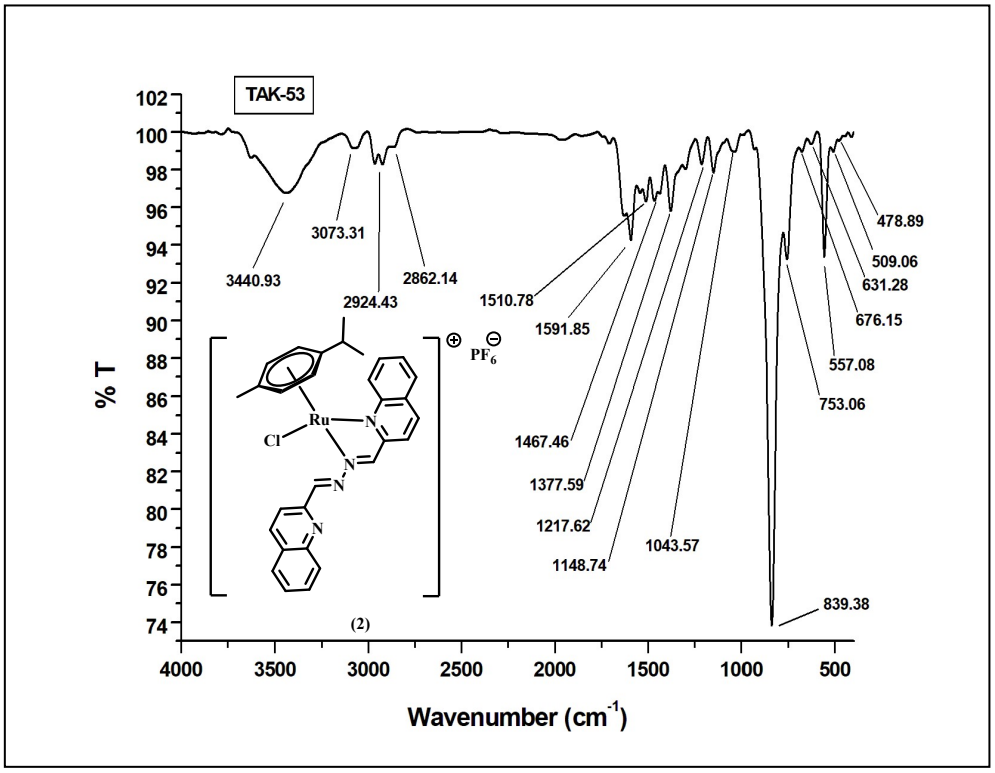

Fig. S1 IR spectrum of **pCYRuL** recorded using KBr disc technique.

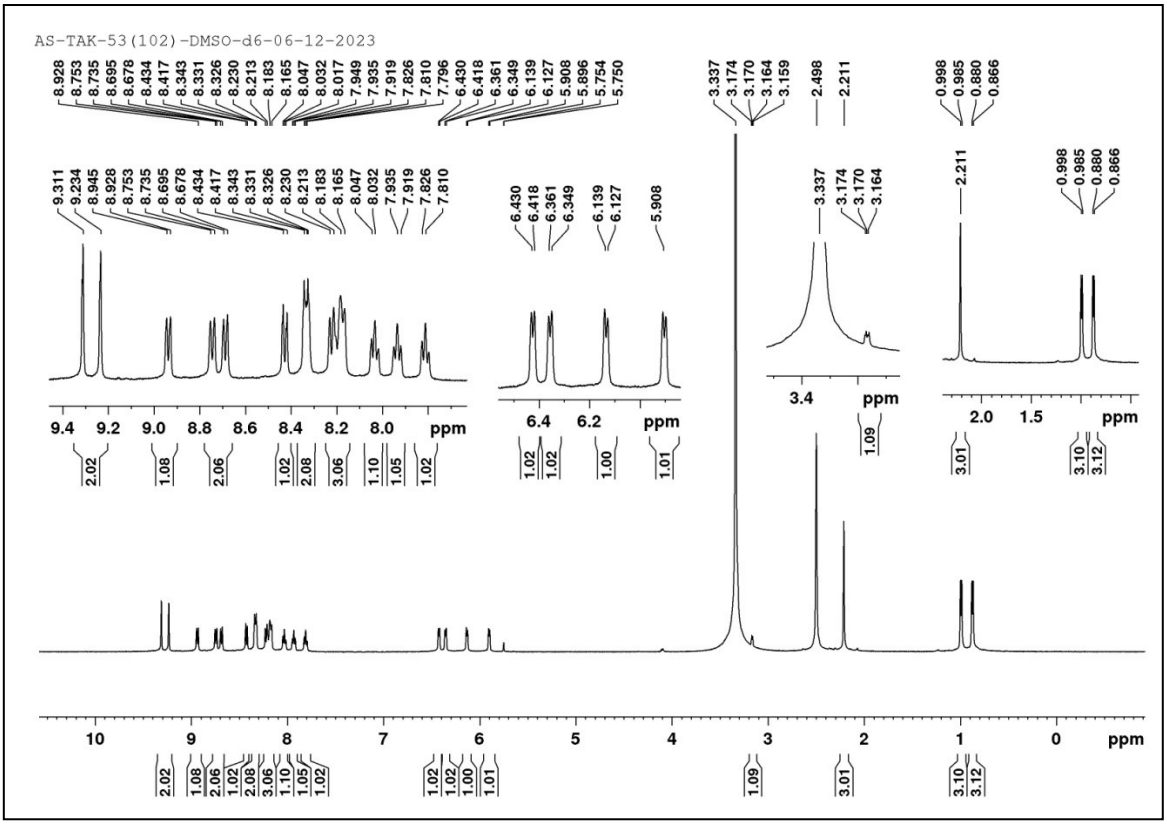

Fig. S2. ^{1}H-NMR spectrum of **pCYRuL** recorded in DMSO-d_6.

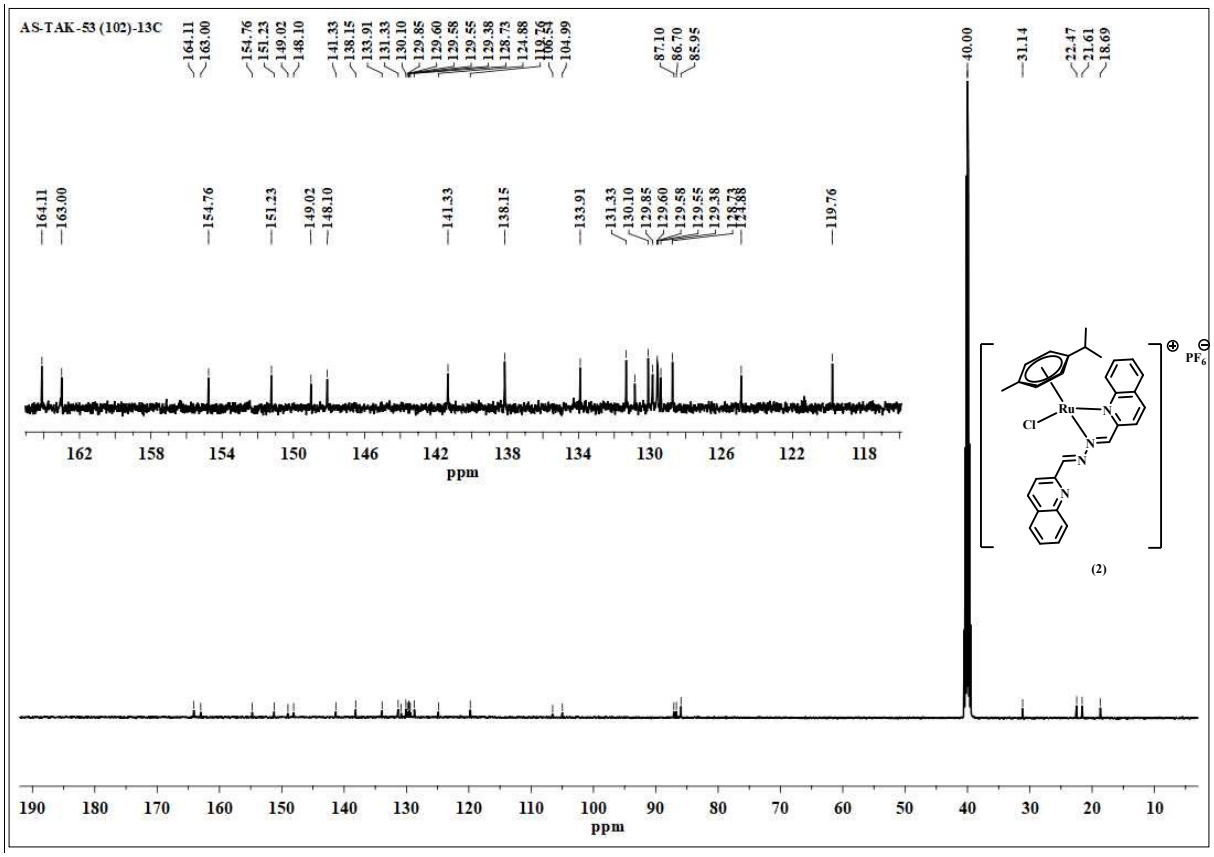

Fig. S3. ^{13}C-NMR spectrum of **pCYRuL** recorded in DMSO-d$_6$.

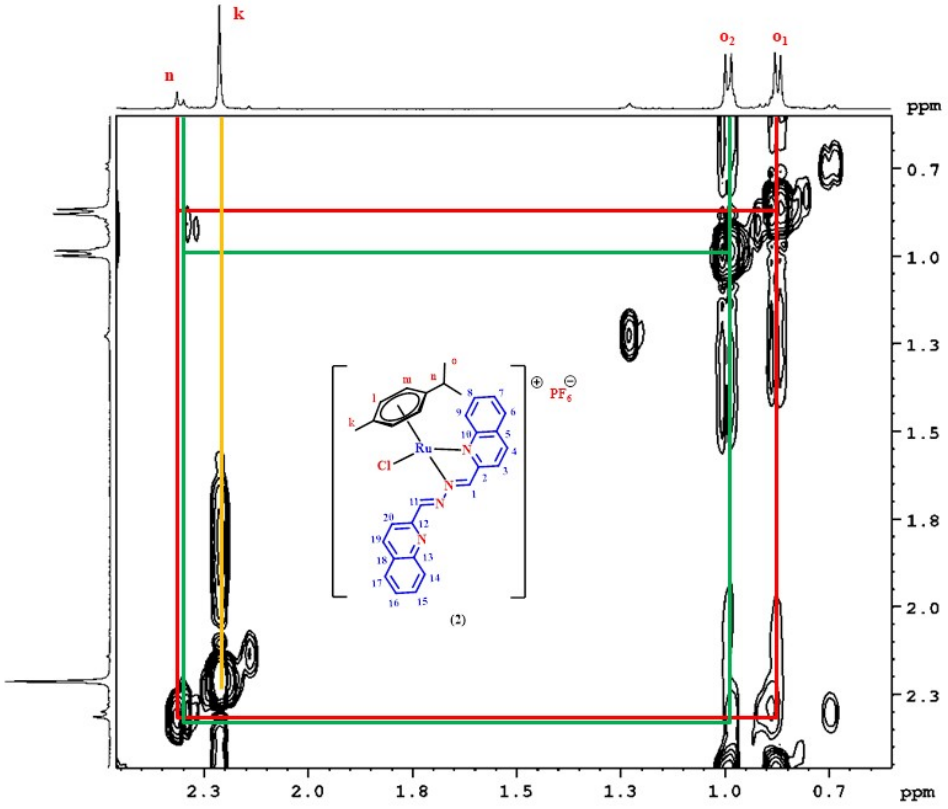

Fig. S4. Aliphatic region of ^{1}H-^{1}H-COSY NMR spectrum of **pCYRuL** recorded in DMSO-d$_6$.

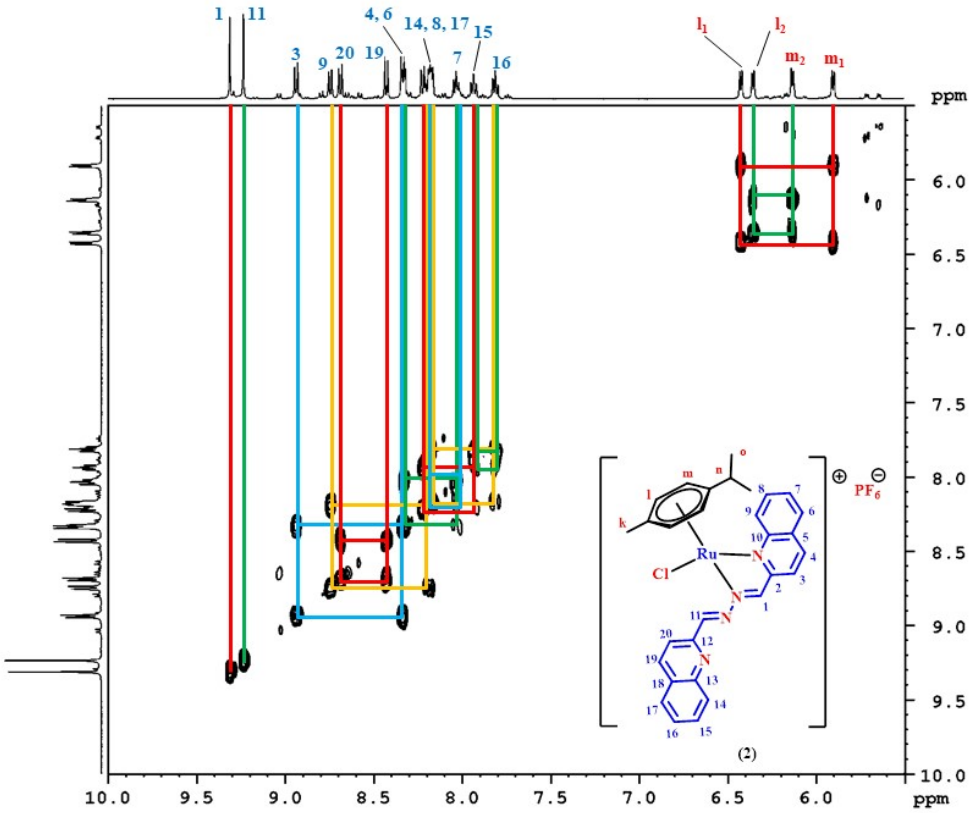

Fig. S5. Aromatic region of the ^{1}H-^{1}H-COSY NMR spectrum of **pCYRuL** recorded in DMSO-d_6.

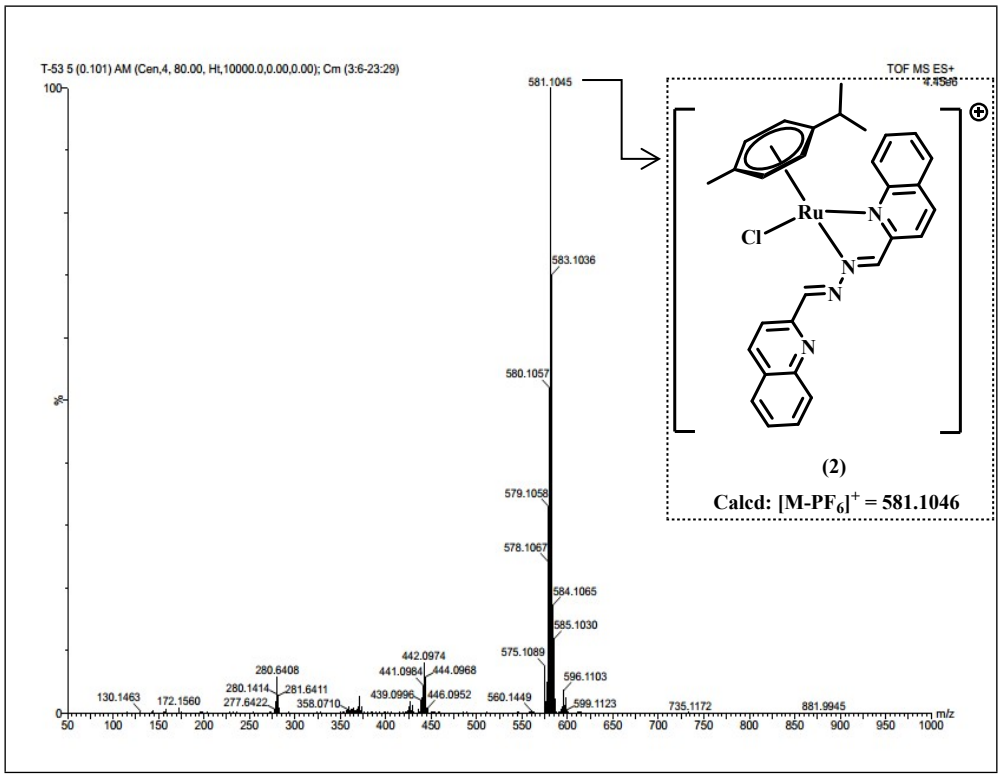

Fig. S6. ESI-Mass spectrum of **pCYRuL** recorded in methanol.

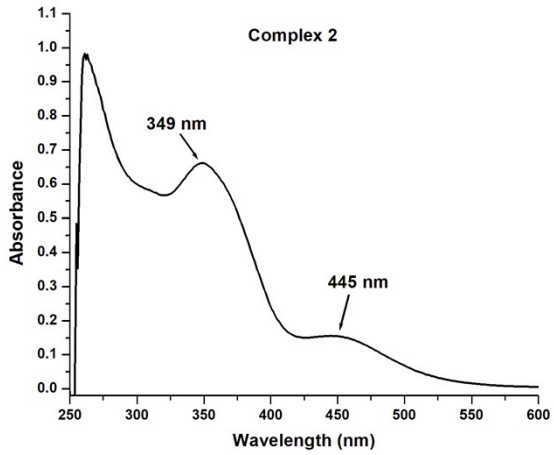

Fig. S7. UV-Vis absorption spectra of **pCYRuL** [30 μM] recorded in DMSO at 298 K.

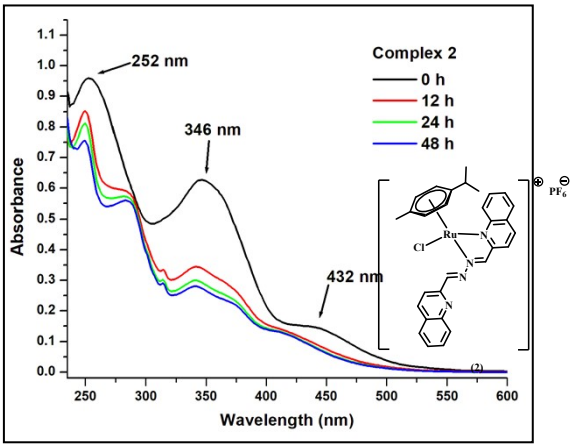

Fig. S8. UV-Visible absorption spectra of **pCYRuL** (30 μM) recorded in 4% DMSO-PBS (pH ~ 7.4) after 0, 12, 24 and 48 h at 298 K.

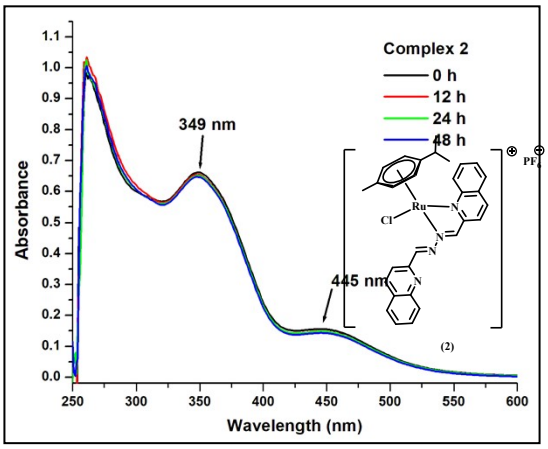

Fig. S9. UV-Visible absorption spectra of **pCYRuL** (30 μM) recorded in DMSO after 0, 12, 24 and 48 h at 298 K.

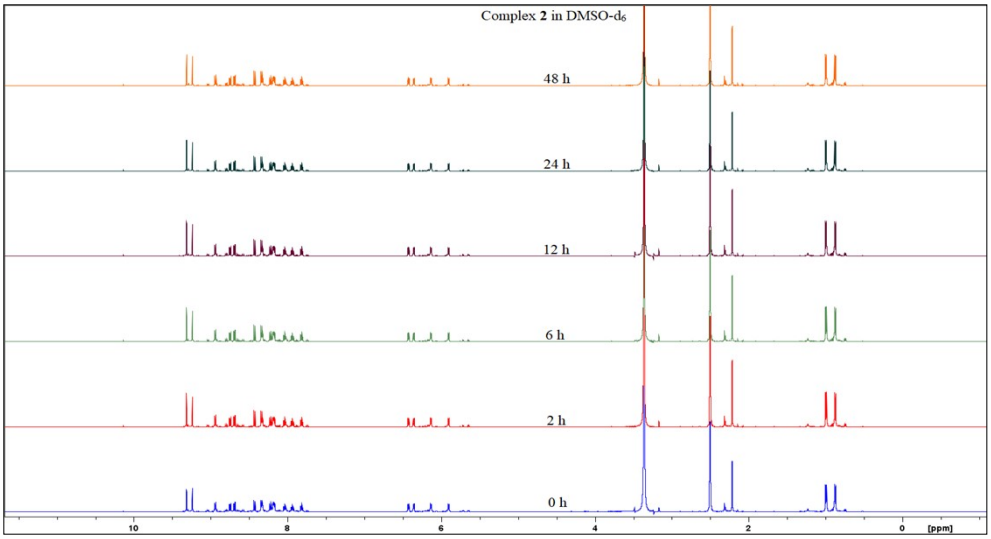

Fig. S10. ^{1}H-NMR spectrum of **pCYRuL** recorded in DMSO-d_6 after 0, 0.5, 2, 6, 12, 24 and 48 h at 298 K.

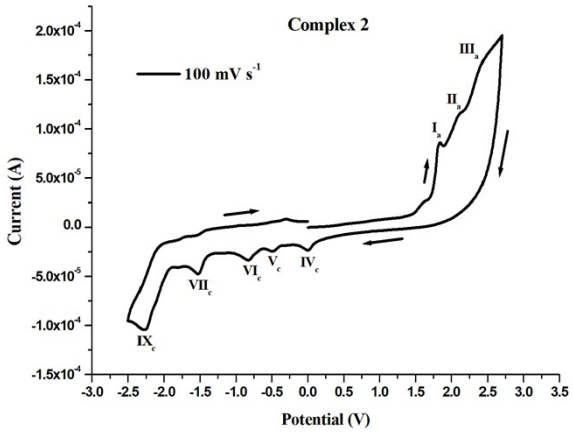

Fig. S11. Cyclic voltammograms of **pCYRuL** (1 mM) solution in CH_3CN with 0.1 M [nBu4N][ClO4] at scan rates: 100 mV s-1 at room temperature.

Table S1: Data obtained from the cyclic voltammetry analyses of **pCYRuL** at the scan rate of 100 mV s-1.

Complexes	EpIa (V)	EpIIa (V)	EpIIIa (V)	EpIVc (V)	EpVa (V)	EpVc (V)	ΔEpV (V)	EpVIc (V)	EpVIIc (V)	EpVIIIc (V)	EpIXc (V)
pCYRuL	1.89	2.16	2.50	0.05	-	-0.44	-	-0.77	-1.47	-	-2.22

Table S2: Toxicity results of pCYRuL in various cancer cells. The tests were conducted in triplicate.

	Type of Cancer Cells				
	Prostate (PC3) (IC50 µM)	Liver (HePG2) (IC50 µM)	Breast (MCF 7) (IC50 µM)	Ovarian (A0287) (IC50 µM)	Pancreatic (PANC1) (IC50 µM)
pCYRuL	0.71	14.72	18.84	8.02	10.73

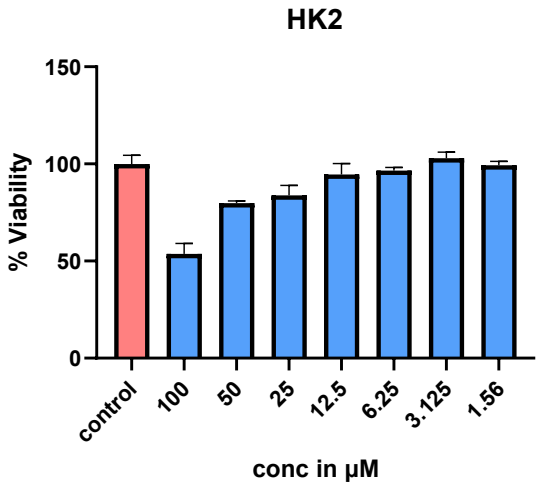

Fig. S12. Toxicity results of pCYRuL in HK-2 cells. The tests were conducted in triplicate.

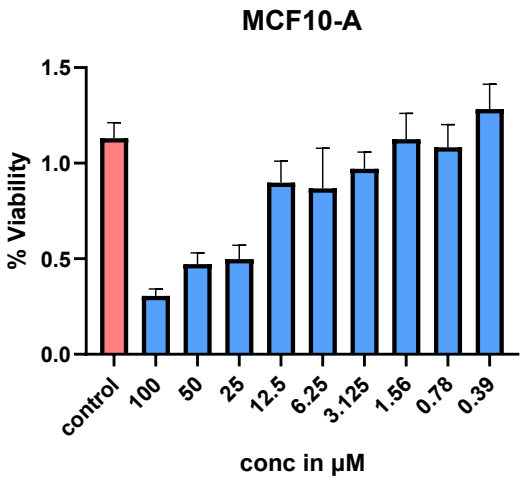

Fig. S13. Toxicity results of pCYRuL in MCF10-A cells. The tests were conducted in triplicate.

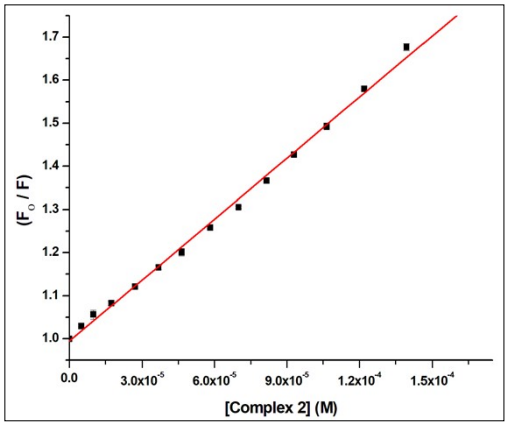

Fig. S14. Stern-Volmer plot for the calculation of quenching constant (K_{SV}) associated with the titration of EthBr-DNA and **pCYRuL** at 298 K.

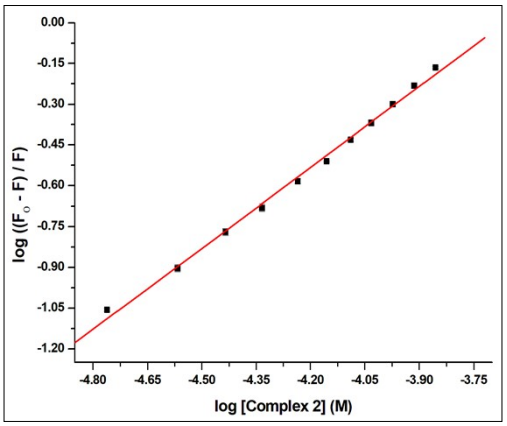

Fig. S15. Scatchard plot for the calculation of association constant (K_a) related with the interaction of EthBr-DNA and **pCYRuL** at 298 K.

Table S3. Data from the emission spectroscopic studies on the DNA binding ability of complexes **1-3**.

Complexes	Quenching constant (K_{SV}) (M^{-1})	Association Constant (K_a) (M^{-1})	No. of binding site (n)
pCYRuL	$4.72 \pm 0.017 \times 10^3$	$4.34 \pm 0.09 \times 10^3$	0.99
Ru (p-cymene) dimer {Khan, 2020 #5893}	$1.35 \pm 0.027 \times 10^3$	$4.01 \pm 0.67 \times 10^2$	0.85

1. C. Ichimura, Y. Shiraishi and T. Hirai, *Journal of Photochemistry and Photobiology A: Chemistry*, 2011, **217**, 253-258.
2. M. A. Bennett and A. K. Smith, *Journal of the Chemical Society, Dalton Transactions*, 1974, 233-241.
3. J. Tönnemann, J. Risse, Z. Grote, R. Scopelliti and K. Severin, *European Journal of Inorganic Chemistry*, 2013, **2013**, 4558-4562.
4. N. Elgrishi, K. J. Rountree, B. D. McCarthy, E. S. Rountree, T. T. Eisenhart and J. L. Dempsey, *Journal of Chemical Education*, 2018, **95**, 197-206.
5. H.-K. Liu and P. J. Sadler, *Accounts of chemical research*, 2011, **44**, 349-359.
6. F. M. Almes, *Biochemistry*, 1993, **32**, 4246-4253.
7. A. Kumar, A. Kumar, R. K. Gupta, R. P. Paitandi, K. B. Singh, S. K. Trigun, M. S. Hundal and D. S. Pandey, *Journal of Organometallic Chemistry*, 2016, **801**, 68-79.
8. K. Ghosh, P. Kumar, N. Tyagi and U. P. Singh, *Inorganic chemistry*, 2010, **49**, 7614-7616.
9. S. Baskaran, M. Murali Krishnan and M. N. Arumugham, *Journal of Coordination Chemistry*, 2015, **68**, 4395-4407.
10. R. Pettinari, F. Marchetti, A. Petrini, C. Pettinari, G. Lupidi, B. Fernández, A. R. Diéguez, G. Santoni and M. Nabissi, *Inorganica Chimica Acta*, 2017, **454**, 139-148.
11. S. Jain, T. A. Khan, Y. P. Patil, D. Pagariya, N. Kishore, S. Tapryal, A. D. Naik and S. G. Naik, *Journal of Photochemistry and Photobiology B: Biology*, 2017, **174**, 35-43.